 doi:10.20944/preprints202204.0191.v1

*Article*

# Three-dimensional theoretical model for soil arching with inclined slip surfaces

**Qizhi Chen [1], Luju Liang [2]*, Changjie Xu [3,4] and Baoping Zou [5]**

[1] School of Civil Engineering and Architecture, Zhejiang University of Science Technology; chenqizhi@zust.edu.cn
[2] School of Engineering, Zhejiang University City College; lianglj@zucc.edu.cn
[3] Engineering Research Development Centre for Underground Technology of Jiangxi Province, East China Jiaotong University; xucj@zju.edu.cn
[4] Research Centre of Coastal and Urban Geotechnical Engineering, Zhejiang University; xucj@zju.edu.cn
[5] School of Civil Engineering and Architecture, Zhejiang University of Science Technology; zoubp@zust.edu.can
* Correspondence: lianglj@zucc.edu.cn

**Abstract:** Terzaghi proposed two-dimensional (2D) arching theory through trapdoor tests based on the assumption of a vertical slip surfaces. However, the original 2D assumption is different from a real three-dimensional (3D) excavation condition and an actual slip surfaces caused by downward movement of a trapdoor is an inclined surface. Therefore, a 3D theoretical model was proposed in this study considering inclined slip surfaces. Horizontal thin layer differential element method was used to obtain the loosening soil pressure. Using the 3D theoretical model, the effects of buried depth ratio of loose area, length of loose area, soil parameters, and lateral earth pressure coefficient were investigated. The loosening earth pressure was highly affected by inclination angle of slip surface, buried depth ratio and length of loose area. Neglecting the inclined slip surface will underestimate the value of the loosening earth pressure, which will lead to the insecurity of the design. Loosening earth pressure calculated by this study was also compared with trapdoor tests. Results from this study was in good agreement with the experimental results. Compared with the traditional 2D solution, results from this study can more accurately analyze the soil arching effect in 3D excavation cases.

**Keywords:** Arching effect; Trapdoor; Inclined slip surface; Excavation

## 1. Introduction

Load transformation from yielding part of soil to adjacent part is known as soil arching effect, which plays an important role in the design of various geotechnical infrastructures [1]. Terzaghi's trapdoor test was an important milestone in the development of theories on soil arching. After that, many researchers have performed trapdoor test to study the soil arching effect [2–9]. Terzaghi then proposed two-dimensional (2D) arching theory through trapdoor tests using horizontal thin layer differential element analysis method based on the assumption of vertical slip surfaces.

Terzaghi's solution is widely used by the practicing engineering in filed applications because of its simplicity. However, the assumption that the slip surfaces is vertical may not be suitable for all kinds of soil and engineering conditions. Inclined slip surfaces on a trapdoor been observed in many experimental studies. Evans [4] and Tien [10] observed non vertical slip surfaces in their model tests. Costa et al. [7] carried out a series of trapdoor tests. Different slip surfaces were observed in tests including the final slip surface inclined to the outside of trapdoor. Papamichos et al. [11] conducted circular retracting Trapdoor model testes and the results showed that slip surfaces tend to have a trapezoid shape in shallower cover soils. Pardo and Sáez [12] carried out trapdoor model test and corresponding numerical simulation. It was found that the final slip surfaces were slightly

outward inclined in the tests and simulation results. Rui et al. [13] found three kinds of soil-arching evolution patterns in Trapdoor tests and described the inclination of the slip surfaces.

Many scholars have carried out relevant research by using the assumption of inclined slip surfaces. Shukla and Sivakugan [14] presented arching theory assuming basin slip surfaces close to the actual slip surfaces. British Standards [15] also adopted this kind of slip surfaces. Gong et al. [16] proposed a method for calculating the loosening earth pressure based on the ellipsoid theory of particle flows using an ellipse slip face. Lai et al. [17] proposed analytical solutions for shallow cohesive soils overlying trench voids under various slip surfaces in the shape of vertical, trapezoid, spiral or arching.

Most studies on soil arching effect are based on 2D condition, but in practical engineering soil arching effect happens under three-dimensional (3D) conditions. For example, during the process of tunnel excavation, stress transfer phenomenon caused by soil arching effect happens not only in the transverse section, but also in the longitudinal section. Many experiment and theoretical studies have been performed under 3D condition. Hewlett and Randolph [18] established a 3D analytical model of a circle-shaped arch for a plane-strain geometry. Adachi et al. [19] performed three-dimensional trapdoor experiments to study the mechanical behavior in tunnel excavations. Li et al. [20] formulated a three dimensional analytical solution to evaluate stresses in backfilled vertical narrow openings using vertical slip surfaces. Son [21] deduced the solution of loose earth pressure in the case of 3D with inclined slip surfaces, but there were some omissions in the derivation. Chevalier and Otani [22] presented experimental and numerical studies of the Trapdoor problem in 3D with rectangular Trapdoor. Ma and Huang [23] study the 3D effect of soil arching effect in piled-embankments by discrete element simulation.

However, there are still few theoretical studies on the 3D soil arching effect considering the inclined slip surface. Therefore, a 3D theoretical model was proposed in this study considering inclined slip surfaces. Horizontal thin layer differential element method was used to obtain the loosening soil pressure. The 3D solution is validated in the degenerate case by traditional analytical solutions. Using the 3D theoretical model, the effects of buried depth ratio of loose area, length of loose area, soil parameters, and lateral earth pressure coefficient were investigated. Results from this study was in good agreement with the experimental results. Compared with the traditional two-dimensional solution, results from this study can more accurately analyze the soil arching effect in 3D excavation cases.

## 2. Derivation of 2D theoretical model for soil arching with inclined slip surfaces

Terzaghi's formulation [1] is based on the equilibrium of a thin horizontal differential element of a soil mass. Several assumptions were made in Terzaghi's formulation. The soil was assumed as homogeneous, isotropic and semi-infinite Mohr-Coulomb material. The slip surfaces between loose area and stable area were assumed as vertical. And the shear strength on slip surfaces were fully mobilized. Terzaghi's formulation is shown as follows:

$$\sigma_v = \frac{B\gamma - 2c}{2K\tan\varphi}\left(1 - e^{-2K\tan\varphi(z/B)}\right) + q \cdot e^{-2K\tan\varphi(z/B)} \quad (1)$$

where $\sigma_v$ is vertical stress, $z$ is the depth of soil differential element, $\gamma$ is the unit weight of soil, $c$ is the cohesive of soil, $\phi$ is the internal friction angle of soil, $B$ is the width of loose zone induced by excavation, $K$ is the coefficient of earth pressure.

Shukla and Sivakugan [14] made an attempt to consider slip surfaces closer to the actual slip surfaces in the analysis in 2D condition as shown in Figure 1 The forces acting on the soil differential element in 2D condition can be seen in Figure 2.

Preprints (www.preprints.org) | NOT PEER-REVIEWED | Posted: 20 April 2022 doi:10.20944/preprints202204.0191.v1



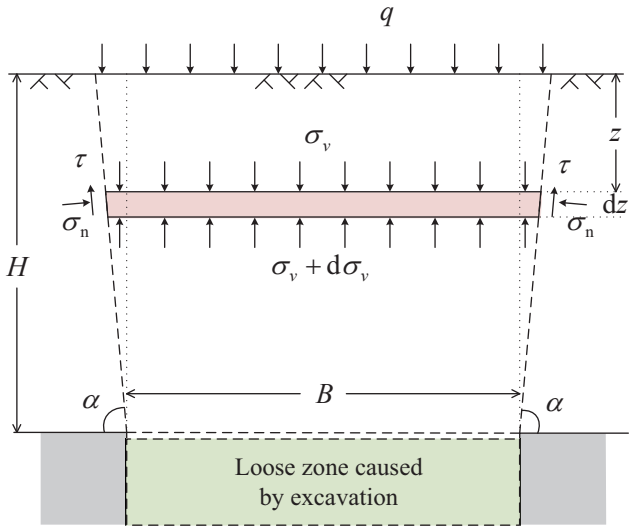


**Figure 1.** Inclined slip surfaces along with soil differential element subjected to stresses in 2D condition.

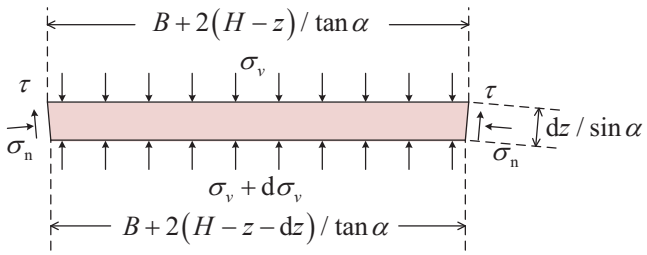


**Figure 2.** Forces acting on the soil differential element in 2D condition.

Assuming that the failure of slip surface follows Mohr-Coulomb failure criterion, vertical equilibrium equation of soil differential element can be obtained according to the vertical force balance.

$$\begin{aligned}&\gamma\left[B+\tfrac{2(H-z)}{\tan\alpha}-\tfrac{\mathrm{d}z}{2\tan\alpha}\right]\mathrm{d}z=(\sigma_{\mathrm{v}}+\mathrm{d}\sigma_{\mathrm{v}})\left[B+\tfrac{2(H-z-\mathrm{d}z)}{\tan\alpha}\right]\\&-\sigma_{\mathrm{v}}\left[B+\tfrac{2(H-z)}{\tan\alpha}\right]+2(c+\sigma_{\mathrm{n}}\tan\varphi)\mathrm{d}z+2\sigma_{\mathrm{n}}\cos\alpha\tfrac{\mathrm{d}z}{\sin\alpha}\end{aligned}\tag{2}$$

where $\alpha$ is the angle between slip surface and horizontal direction, $\sigma_{\mathrm{n}}$ is the normal stress perpendicular to slip surface.

By simplifying and ignoring the second-order infinitesimal, it can be obtained from equation (2):

$$\gamma B-2c+\frac{2\gamma(H-z)}{\tan\alpha}+\frac{2\sigma_{\mathrm{v}}}{\tan\alpha}-2\sigma_{\mathrm{n}}\left(\tan\varphi+\frac{1}{\tan\alpha}\right)=\frac{\mathrm{d}\sigma_{\mathrm{v}}}{\mathrm{d}z}\left[B+\frac{2(H-z)}{\tan\alpha}\right]\tag{3}$$

According to the equilibrium conditions at both ends of the differential element:

$$\sigma_{\mathrm{n}}=\sigma_{\mathrm{v}}\left(\cos^2\alpha+K\sin^2\alpha\right)\tag{4}$$

Substitute (4) into (3) will get an ordinary differential equation:

$$\begin{aligned}&\tfrac{\mathrm{d}\sigma_{\mathrm{v}}}{\mathrm{d}z}[B\tan\alpha+2(H-z)]=(\gamma B-2c)\tan\alpha+2\gamma(H-z)+2\sigma_{\mathrm{v}}\\&-2\sigma_{\mathrm{v}}\left(\cos^2\alpha+K\sin^2\alpha\right)(\tan\alpha\tan\varphi+1)\end{aligned}\tag{5}$$

Preprints (www.preprints.org) | NOT PEER-REVIEWED | Posted: 20 April 2022 doi:10.20944/preprints202204.0191.v1



Defining $P$, $Q$, $R$ and $S$ as follows:

$$P = -2/\tan\alpha \tag{6a}$$

$$Q = B + 2H/\tan\alpha \tag{6b}$$

$$R = (\gamma B - 2c) + 2\gamma H/\tan\alpha \tag{6c}$$

$$S = \left(\cos^2\alpha + K\sin^2\alpha\right)(P - 2\tan\varphi) - P \tag{6d}$$

The general solution of the differential equation can be obtained as follows:

$$\sigma_{\mathrm{v}} = \lambda(Pz + Q)^{S/P} + \frac{PS\gamma z + PQ\gamma - PR + RS}{S(P - S)} \tag{7}$$

The boundary condition is shown as follows:

$$z = 0, \sigma_{\mathrm{v}} = q \tag{8}$$

The parameter $\gamma$ can be solved according to the boundary condition. The earth pressure can be obtained as follows:

$$\sigma_{\mathrm{v}} = \left[\frac{q}{Q^{S/P}} - \frac{PQ\gamma - PR + RS}{S(P - S)Q^{S/P}}\right](Pz + Q)^{S/P} + \frac{PS\gamma z + PQ\gamma - PR + RS}{S(P - S)} \tag{9}$$

## 3. Derivation of 3D theoretical model for soil arching with inclined slip surfaces

This study expands Shukla and Sivakugan [14] 2D theoretical model for soil arching with inclined slip surfaces to 3D conditions. Figure 3 shows the assumed inclined slip surfaces along with soil differential element subjected to stresses. It is also assumed that the soil is homogeneous, isotropic, and semi-infinity.

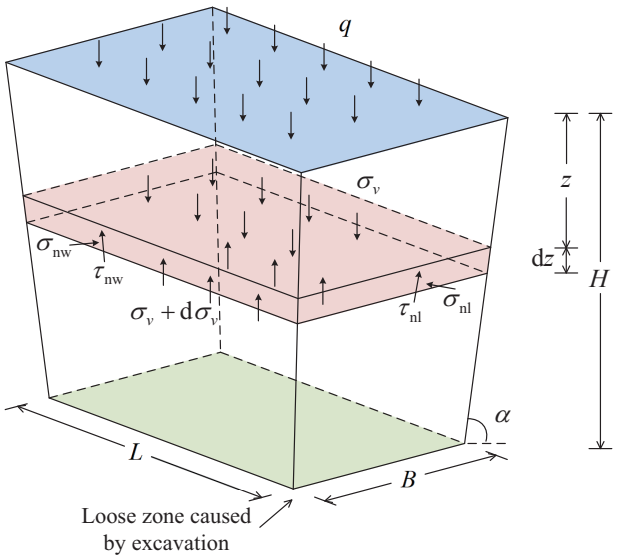


**Figure 3.** Inclined slip surfaces along with soil differential element subjected to stresses in 3D condition.

Preprints (www.preprints.org) | NOT PEER-REVIEWED | Posted: 20 April 2022 doi:10.20944/preprints202204.0191.v1



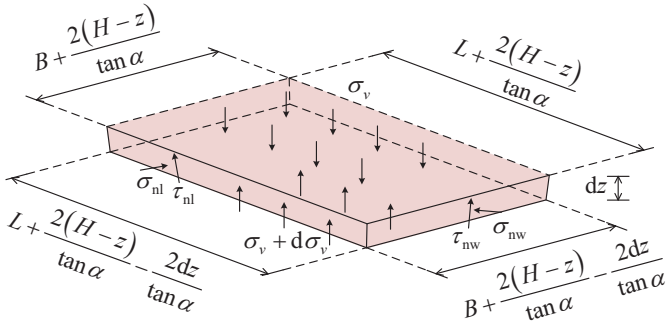


**Figure 4.** Forces acting on the soil differential element in 3D condition.

The 3D model for soil arching with inclined slip surfaces is shown in Figure 4 The slip surfaces incline outside along excavation loosening zone. Assuming that the failure of slip surface follows Mohr-Coulomb failure criterion, vertical equilibrium equation of soil differential element can be obtained according to the vertical force balance.

$$\begin{aligned}
&\gamma\left[BL+\tfrac{2(B+L)(H-z)}{\tan\alpha}+\tfrac{4(H-z)^2}{\tan\alpha}\right]\mathrm{d}z=\tfrac{2(B+L)(H-z)}{\tan\alpha}\mathrm{d}\sigma_\mathrm{v}\\
&+\tfrac{4(H-z)^2}{\tan^2\alpha}\mathrm{d}\sigma_\mathrm{v}-\tfrac{2(B+L)\sigma_\mathrm{v}}{\tan\alpha}\mathrm{d}z-\tfrac{8(H-z)\sigma_\mathrm{v}}{\tan^2\alpha}\mathrm{d}z+BL\mathrm{d}\sigma_\mathrm{v}\\
&+\tfrac{2\sigma_\mathrm{nw}}{\tan\alpha}\left(B+\tfrac{2(H-z)}{\tan\alpha}-\tfrac{\mathrm{d}z}{\tan\alpha}\right)\mathrm{d}z+2c\left(B+\tfrac{2(H-z)}{\tan\alpha}-\tfrac{\mathrm{d}z}{\tan\alpha}\right)\mathrm{d}z\\
&+\tfrac{2\sigma_\mathrm{nl}}{\tan\alpha}\left(L+\tfrac{2(H-z)}{\tan\alpha}-\tfrac{\mathrm{d}z}{\tan\alpha}\right)\mathrm{d}z+2c\left(L+\tfrac{2(H-z)}{\tan\alpha}-\tfrac{\mathrm{d}z}{\tan\alpha}\right)\mathrm{d}z\\
&+2\sigma_\mathrm{nw}\tan\varphi\left(B+\tfrac{2(H-z)}{\tan\alpha}-\tfrac{\mathrm{d}z}{\tan\alpha}\right)\mathrm{d}z\\
&+2\sigma_\mathrm{nl}\tan\varphi\left(L+\tfrac{2(H-z)}{\tan\alpha}-\tfrac{\mathrm{d}z}{\tan\alpha}\right)\mathrm{d}z
\end{aligned}\tag{10}$$

where $\gamma$ is the unit weight of soil, $c$ is the cohesive of soil, $\phi$ is the internal friction angle of soil, $B$ is the width of loose zone induced by excavation, $H$ is the depth of loosening soil, $L$ is the length of loose zone induced by excavation, $\alpha$ is the angle between slip surface and horizontal direction, $z$ is the depth of soil differential element, $\sigma_\mathrm{v}$ is vertical stress, $\sigma_\mathrm{nw}$ is normal stress perpendicular to the width direction, $\sigma_\mathrm{nl}$ is the normal stress perpendicular to the length direction.

According to the equilibrium conditions at both ends of the differential element, it can be obtained:

$$\sigma_\mathrm{nw}=\sigma_\mathrm{v}\left(\cos^2\alpha+K_\mathrm{w}\sin^2\alpha\right)\tag{11}$$

$$\sigma_\mathrm{nl}=\sigma_\mathrm{v}\left(\cos^2\alpha+K_\mathrm{l}\sin^2\alpha\right)\tag{12}$$

where $K_\mathrm{w}$ is the coefficient of earth pressure perpendicular to the width direction, $K_\mathrm{l}$ is the coefficient of earth pressure perpendicular to the length direction. Substitute equations (11) and (12) into equation (10). By simplifying and ignoring the second-order infinitesimal, the ordinary differential equation of vertical force on soil differential element can be obtained.

$$\begin{aligned}
&\gamma\left[BL+\tfrac{2(B+L)(H-z)}{\tan\alpha}+\tfrac{4(H-z)^2}{\tan\alpha}\right]-2c\left(B+L+\tfrac{4(H-z)}{\tan\alpha}\right)\\
&-\sigma_\mathrm{v}\left\{\begin{array}{l}
\tfrac{2\left(\cos^2\alpha+K_\mathrm{w}\sin^2\alpha\right)}{\tan\alpha}\left(B+\tfrac{2(H-z)}{\tan\alpha}\right)\\
+\tfrac{2\left(\cos^2\alpha+K_\mathrm{l}\sin^2\alpha\right)}{\tan\alpha}\left(L+\tfrac{2(H-z)}{\tan\alpha}\right)\\
+2\left(\cos^2\alpha+K_\mathrm{w}\sin^2\alpha\right)\tan\varphi\left(B+\tfrac{2(H-z)}{\tan\alpha}\right)\\
+2\left(\cos^2\alpha+K_\mathrm{l}\sin^2\alpha\right)\tan\varphi\left(L+\tfrac{2(H-z)}{\tan\alpha}\right)\\
-\tfrac{2(B+L)}{\tan\alpha}-\tfrac{8(H-z)}{\tan^2\alpha}
\end{array}\right\}\\
&=\left(BL+\tfrac{2(B+L)(H-z)}{\tan\alpha}+\tfrac{4(H-z)^2}{\tan^2\alpha}\right)\tfrac{\mathrm{d}\sigma_\mathrm{v}}{\mathrm{d}z}
\end{aligned}\tag{13}$$

Preprints (www.preprints.org) | NOT PEER-REVIEWED | Posted: 20 April 2022 doi:10.20944/preprints202204.0191.v1



The boundary condition is the surface load $q$. So the boundary condition equation is expressed as follows:

$$z = 0, \sigma_v = q \tag{14}$$

According to the boundary condition equation (14), the only solution of ordinary differential equation (13) can be determined. That is to solve the initial value problem of ordinary differential equations. However, the ordinary differential equation (13) is so complex that it is difficult to give the explicit expression of the solution. Therefore, the fourth-order Runge-Kutta method is used to calculate the vertical stress of soil when the depth is z by matlab programming.

The ordinary differential equation (13) can be written as:

$$\frac{d\sigma_v}{dz} = f(z_n, \sigma_{vn}) \tag{15}$$

And the calculation formula of the fourth-order Runge-Kutta method is expressed as follows:

$$\begin{cases} P_1 = f(z_n, \sigma_{vn}) \\ P_2 = f\left(z_n + \frac{i}{2}, \sigma_{vn} + \frac{i}{2}P_1\right) \\ P_3 = f\left(z_n + \frac{i}{2}, \sigma_{vn} + \frac{i}{2}P_2\right) \\ P_4 = f(z_n + i, \sigma_{vn} + iP_3) \\ \sigma_{vn+1} = \sigma_{vn} + \frac{i}{6}(P_1 + 2P_2 + 2P_3 + P_4) \end{cases} \tag{16}$$

where $i$ is the length of integral step and $P_1$, $P_2$, $P_3$, $P_4$ are integral parameters.

An example is used to verify whether the 3D theoretical model for loose earth pressure with inclined slip surfaces is consistent with two dimensional loose earth pressure solution mentioned above. In this example, the following parameters $H$=15m, $B$=3m, $\phi$=35°, $c$=0kPa, $q$=0kPa and $\gamma$=18kN/m$^3$ are used for calculation. In the 3D example the value of $L$ is 1000 m, which is approximately considered to degenerate into a 2D case. The calculation results are shown in Figure 5.

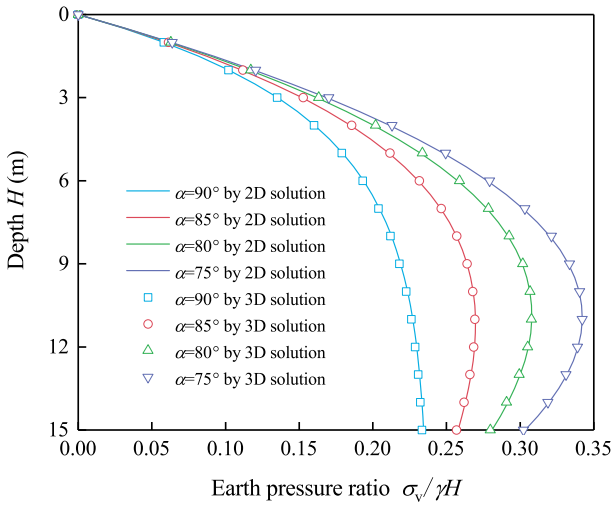


**Figure 5.** Earth pressure ratio versus depth under different angle of slip surface.

It can be obtained from the calculation results that the curve of earth pressure ratio versus depth under different angle of slip surface calculated by degenerated 3D solution is consistent with the results of the 2D solution. Thus the correctness of the 3D solution can be verified.

Preprints (www.preprints.org) | NOT PEER-REVIEWED | Posted: 20 April 2022 doi:10.20944/preprints202204.0191.v1



## 4. Analysis of parameters on loose earth pressure under 3D inclined slip surface condition

In order to study the influence of parameters on loose earth pressure under 3D inclined slip surface condition, a series of cases are carried out. The buried depth ratio of loose zone, the length of loose zone, the soil parameters and the lateral earth pressure coefficient are taken into account, and corresponding analysis is carried out. The parameters for special cases are shown in Table 1.

**Table 1.** The parameters for different cases.

| Cases | $H$ (m) | $B$ (m) | $\phi$ (°) | $L$ (m) | $\alpha$ (°) | $c$ (kPa) | $K_w$ | $K_l$ |
|---|---|---|---|---|---|---|---|---|
| 1 | 10 | 5 | 30 | 10 | variation | 0 | 1 | 1 |
| 2 | 10 | 5 | 30 | variation | variation | 0 | 1 | 1 |
| 3 | variation | 5 | 30 | variation | 85 | 0 | 1 | 1 |
| 4 | 10 | 5 | variation | variation | 85 | 0 | 1 | 1 |
| 5 | 10 | 5 | variation | variation | 85 | variation | 1 | 1 |
| 6 | 10 | 5 | 30 | 10 | 80 | 0 | variation | variation |
| 7 | 10 | 5 | 30 | variation | 80 | 0 | variation | variation |

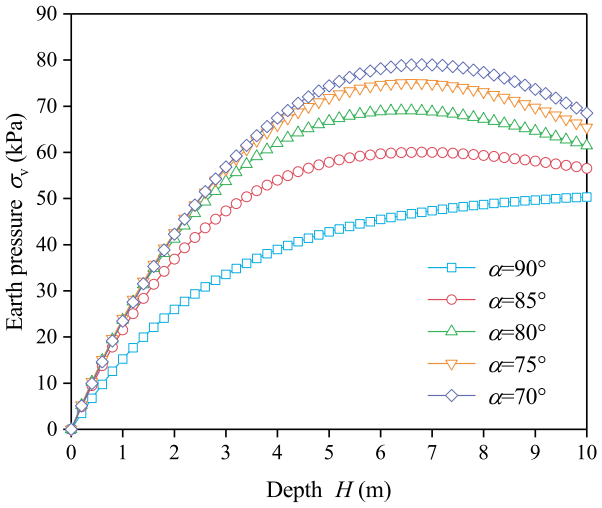


**Figure 6.** Earth pressure versus depth under different angle of slip surface.

In case 1, the earth pressure under different angle of slip surface is calculated and the other parameters in case 1 are consistent. It can be seen from the results shown in Figure 6 that the earth pressure at each depth increases with the decrease of the angle of slip surface. This is mainly because the upward component provided by the shear resistance between slip surfaces decreases when the angle of slip surface decreases. It also can be found that the maximum earth pressure may not occur at the bottom of the soil when the angle of slip surface is small. The maximum earth pressure may occur somewhere in the middle of soil.

The influence of angle of slip surface and aspect ratio of loose area are studied in case 2. The results are shown in Figure 7. The loose earth pressure also shows the same trend as mentioned before under different angles of slip surface.

Preprints (www.preprints.org) | NOT PEER-REVIEWED | Posted: 20 April 2022 doi:10.20944/preprints202204.0191.v1



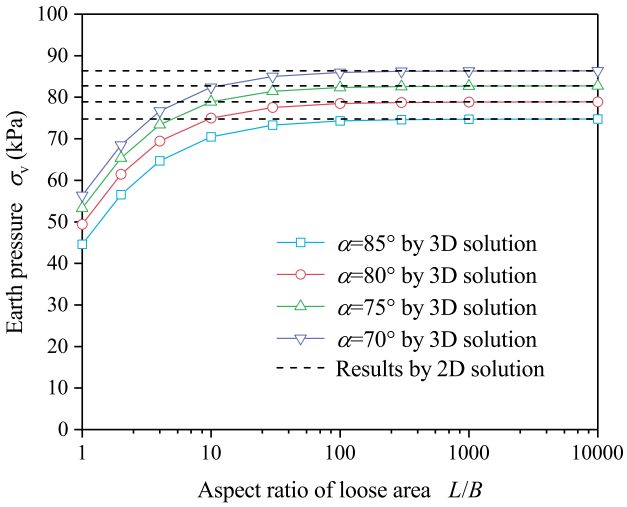


**Figure 7.** Earth pressure versus aspect ratio of loose area under different angle of slip surface.

The depth of soil and the aspect ratio of loose area are studied in case 3. The calculated earth pressure versus aspect ratio of loose area under different angle of slip surface are shown in Figure 8. It can be seen from results that the earth pressure ratio at the bottom of the loose area is small when the buried depth ratio of loose area is large. This is because the stress redistribution is more likely to occur due to the increase of the length of the slip surface when the buried depth ratio is larger. The calculation results under different aspect ratios of loose zone also show the same trend. When $H/B$=1, the loose earth pressure is 42% to 61% of the total self-weight earth pressure under different aspect ratios. When $H/B$=2, it will be 25% to 42% of the total self-weight earth pressure. When $H/B$=3, it will be 17% to 31%, and when $H/B$=4 the loose earth pressure is only 13% to 24% of the total self-weight earth pressure.

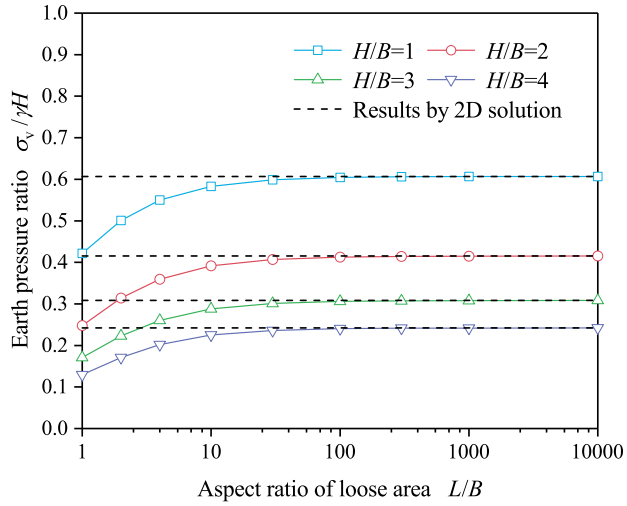


**Figure 8.** Earth pressure ratio versus aspect ratio of loose area under different buried depth ratio of loose area.

The influences of soil parameters are studied in cases 4 and 5. Figure 9 shows the influence of internal friction angle of soil and Fig. 10 shows the influence of cohesion stress of soil. Loose earth pressure is closely related to soil parameters. For frictional soil, the

greater the internal friction angle is, the more obvious the soil arching effect and the smaller the soil pressure will be. For cohesive soil, the larger the internal friction angle and cohesion are, the more obvious the soil arching effect and the smaller the soil pressure will be. The loose earth pressure when internal friction angle is 40 degrees is 53% to 65% of that when internal angle is 25 degrees for different loosing zone aspect ratio. The loose earth pressure when cohesive stress of soil is 15 kPa is 37% to 60% of that when cohesive stress of soil is zero. It can be found that when the aspect ratio of the loose zone is small, the influence of soil parameters on the loose soil pressure is greater than that when the aspect ratio of the loose zone is large.

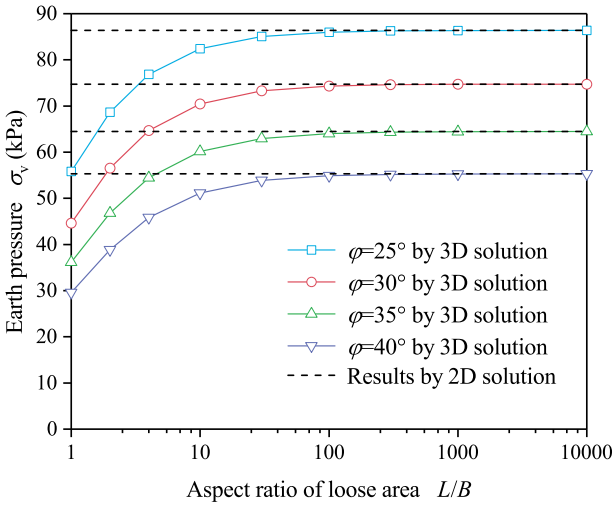


**Figure 9.** Earth pressure versus aspect ratio of loose area under different internal friction angle of soil.

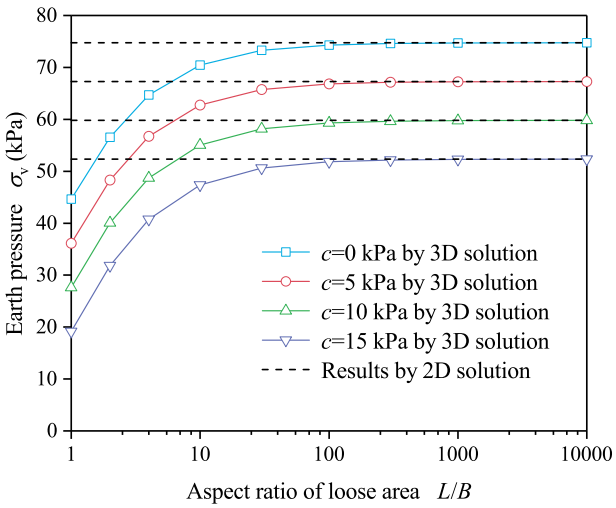


**Figure 10.** Earth pressure versus aspect ratio of loose area under different cohesion stress of soil.

In practical engineering, due to the different geological conditions and boundary conditions of the soil layer, different earth pressure coefficients may exist in the length and width of the excavation loose area. Therefore, the different soil pressure coefficients in

Preprints (www.preprints.org) | NOT PEER-REVIEWED | Posted: 20 April 2022 doi:10.20944/preprints202204.0191.v1



two directions of length and width are considered, and the corresponding calculation and analysis cases 6 and 7 are carried out.

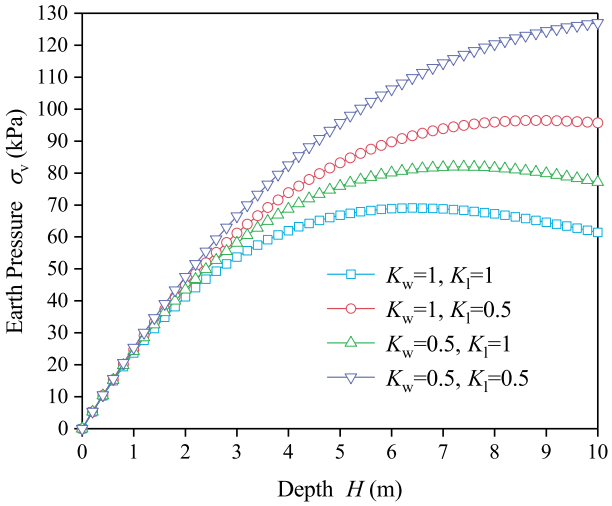


**Figure 11.** Earth pressure versus depth under different earth pressure coefficients.

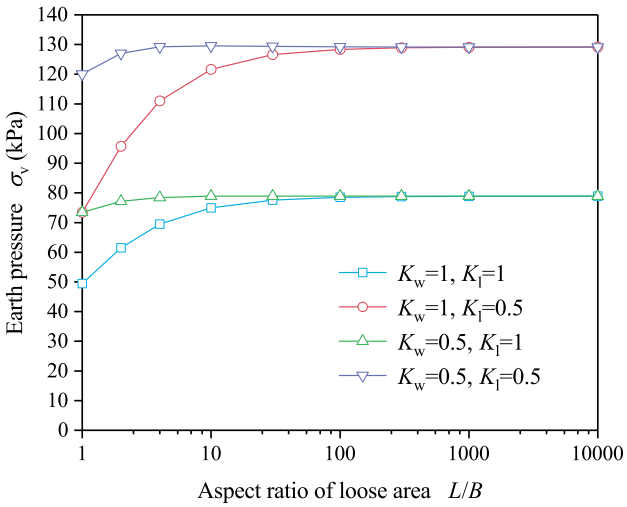


**Figure 12.** Earth pressure versus aspect ratio of loose area under earth different pressure coefficients.

It has been found in the 2D solution that different earth pressure coefficients have great influence on the calculation results of loose earth pressure. The smaller the earth pressure coefficient is, the closer the calculated results are to the total self-weight earth pressure. It can be found in Figures 11 and 12 that this trend still exists in the 3D solution.

In addition, it can be seen from Figure 11 that for the situation of $B$=5 m and $L$=10 m, the earth pressure under $K_w$=1$K_l$=0.5 is greater than that under $K_w$=0.5, $K_l$=1. This is mainly because the length of length direction corresponding to $K_l$ is longer than that of width direction corresponding to $K_w$, so $K_l$ plays a leading role relative to $K_w$. Figure 12 shows that when the aspect ratio of the loose zone is large, it is approximately close to the 2D state, so the soil pressure is mainly affected by $K_l$.

Figuress 7, 8, 9, 10, and 12, show the earth pressure results under different conditions and different aspect ratios of loose zones. It can be found that for all cases, the greater

Preprints (www.preprints.org) | NOT PEER-REVIEWED | Posted: 20 April 2022 doi:10.20944/preprints202204.0191.v1



the aspect ratio of the loose zone is, the greater the loose earth pressure will be. In other words, the traditional 2D solution which cannot consider the sliding surface at both ends will underestimate the soil arching effect and overestimate the loose earth pressure under 3D condition with a small aspect ratio. This will overestimate the loose earth pressure to a certain extent, resulting in inaccurate design.

The calculation results by 2D solution are close to results by 3D solution when the aspect ratio increases. Figure 12 shows that when $L/B$=10, the difference between the results under 2D assumption and 3D assumption is 4.1% when $H/B$=1, the difference is 6.1% when $H/B$=2, the difference is 4.1% when $H/B$=3, and the difference is 7.6% when $H/B$=4. So it can be considered that when $L/B$>10, 2D assumption can be approximately used instead of 3D assumption.

## 5. Comparison with Experimental Tests

Experiment tests results are compared with the results by proposed 3D solution with inclined slip surface. Liang et al. [24] conducted three groups of Trapdoor tests with buried depth ratio $H/B$ equal to 1, 2 and 4, respectively. The width and longitude of Trapdoor in the tests is 0.25 m and 0.5 m, respectively. The internal friction angle of well-graded sands is 31.6°. According to the image of test results, the angle of slip surfaces is considered as 85° in the following calculation. The comparison is shown in Figure 13 It can be seen from the comparison that the calculation results by this paper considering 3D condition is slightly less than that by Terzaghi's solution. The results by 3D solution in this paper is closer to the test results when the buried depth ratio is small. The results by Terzaghi's solution is closer to the test results when the buried depth ratio is large. This is because the front wall of the model test chamber is made by toughened glass plate and the other steel walls of the model test chamber are attached with thin Teflon films. The toughened glass plate and thin Teflon films can be regarded as smooth enough to mitigate the effect of friction. In the case of large buried depth ratio, the 3D solution in this paper treat the front and back wall of the test chamber as slip surface equivalent to the left and right sides, which leads to the smaller results of calculated earth pressure.

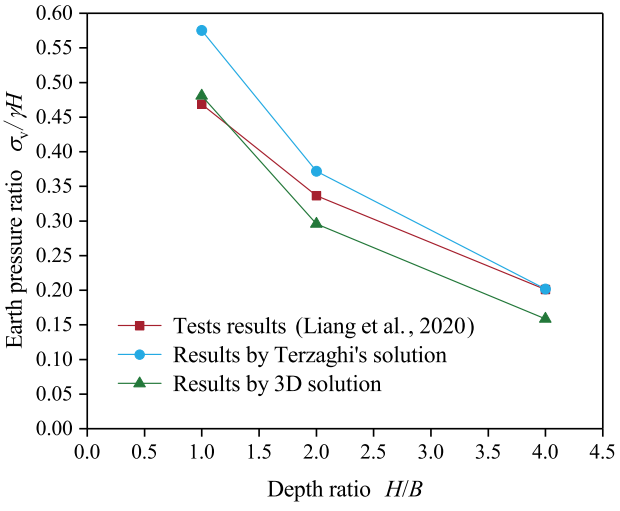


**Figure 13.** Comparison of tests results (Liang *et al.* [24]) and 3D solution.

Adachi et al. [19] developed and performed 3D Trapdoor experiments to clarify the mechanical behavior in tunnel excavations. In the test, a series of adjacent Trapdoors gradually lower down one by one to simulate the soil loosening during shield tunneling. For all Trapdoors, the width of the cross-section is 150 mm. For Trapdoor numbers 1 and 6, the length of the Trapdoors is 200 mm, while it is 150 mm for Trapdoor numbers 2, 3, 4

Preprints (www.preprints.org) | NOT PEER-REVIEWED | Posted: 20 April 2022 doi:10.20944/preprints202204.0191.v1



and 5. The loads applied to the Trapdoors are measured by load cells. The tests results and calculated results by presented solution and Terzaghi's solution for difference buried depth ratio are shown in Figures 14 to 16, respectively. It can be found from results that the earth pressure ratio increases with the increase of the aspect ratio of the loose zone with the test process. The traditional 2D Terzaghi solution can not reflect this trend, but the 3D solution in this paper can reflect this trend. When part of Trapdoors lowered down, such as the aspect ratio of loose zone $L/B$ is 1.33, the earth pressure ratio obtained by Terzaghi's solution have a very large gap with tests results, and the results obtained by the solution in this paper are closer to the tests results. When all of Trapdoors lowered down, such as the aspect ratio of loose zone $L/B$ is 6.67, the earth pressure ratio obtained by Terzaghi's solution and the solution in this paper are both close to the tests results. The comparison between the solution in this paper and the tests results shows that the solution in this paper is more accurate than the traditional 2D solution for calculating loose earth pressure especially in 3D condition.

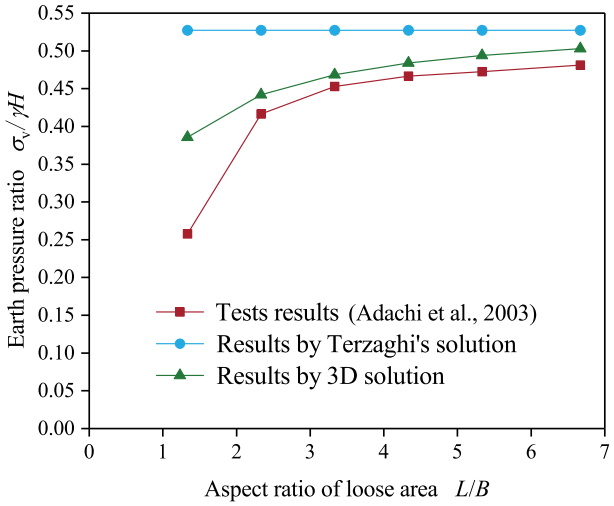


**Figure 14.** Comparison of tests results (Adachi *et al.* [19]) and 3D solution under $H/B$=1.

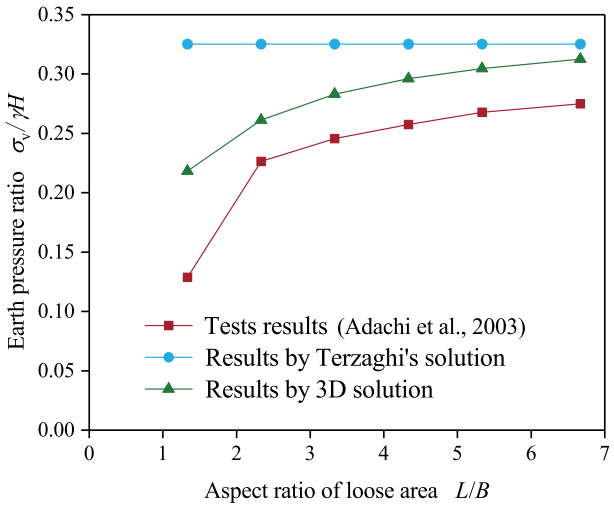


**Figure 15.** Comparison of tests results (Adachi *et al.* [19]) and 3D solution under $H/B$=2.

Preprints (www.preprints.org) | NOT PEER-REVIEWED | Posted: 20 April 2022 doi:10.20944/preprints202204.0191.v1



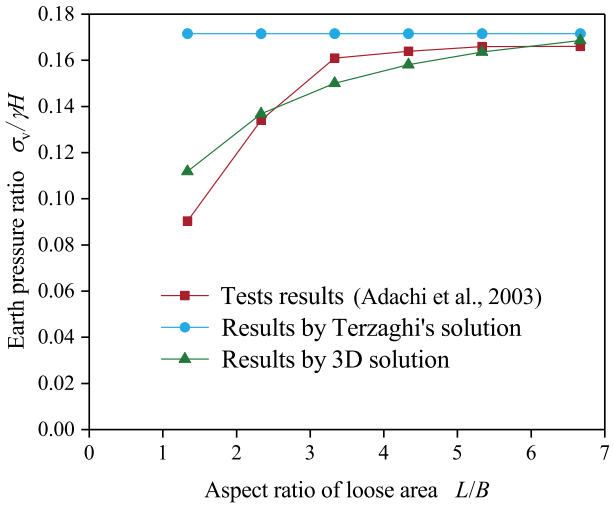


**Figure 16.** Comparison of tests results (Adachi *et al.* [19]) and 3D solution under $H/B$=4.

## 6. Conclusions

Based on Terzaghi's 2D arching theory based on the assumption of a vertical slip surfaces, derivation of 2D and 3D theoretical model for soil arching with inclined slip surfaces are presented in this paper. Horizontal thin layer differential element method was used to obtain the loosening soil pressure. And then the correctness of the 3D solution is verified. Several cases have been done to investigate the effects of buried depth ratio of loose area, length of loose area, soil parameters, and lateral earth pressure coefficient on loose earth pressure. The results by proposed solution are then compared with tests results. Several conclusions can be drawn as follows:

1. The 2D solution with inclined slip surfaces can degenerate into the classical Terzaghi's solution when the angle of inclined slip surfaces is 90 degrees. And the 3D solution with inclined slip surfaces can degenerate into 2D when the length of loose zone trend to be infinite, which can verify the correctness of the solution in this paper.

2. The loose earth pressure is far less than the self-weight earth pressure due to the existence of soil arching effect for both frictional soil and cohesive soil. The earth pressure ratio at each depth increases with the decreases of the angle of inclined slip surfaces. If the angle of slip surfaces closes to 0, the slip surface is approximately parallel to the bottom which means no soil arching effect will happen.

3. The earth pressure ratio decreases with the increase of buried depth ratio. For shallow excavation, the change of the angle of slip surface has little effect on the loose earth pressure. However for deep excavation, the change of the angle of slip surface has great effect on the loose earth pressure. Using traditional Terzaghi's solution with the assumption of vertical slip surfaces will underestimate the value of loose earth pressure for deep excavation condition. It will cause unsafe in design, which needs to be paid attention to in the engineering practice.

4. The soil arching effect is closely related to soil parameters. The larger the internal friction angle and cohesion of soil, the smaller the value of loose earth pressure. The smaller the earth pressure coefficient is, the closer the calculated result is to the self-weight earth pressure. If the earth pressure coefficients in the length and width directions of the excavation loose area are different, the influence of the earth pressure coefficients in the two directions on the results also depends on the aspect ratio of the excavation loose area.

5. For the 3D soil arching effect with small aspect ratio, the 2D solution will underestimate the soil arching effect and overestimate the loose earth pressure, resulting in conservative design. The 2D assumption can be approximately used instead of the 3D assumption when the aspect ratio $L/B$>10.

6. The loose earth pressure results by 3D solution in this paper is in good agreement with the experimental results. Compared with the traditional 2D solution, the solution in this paper can analyze and calculate the soil arching effect more accurately.

**Funding:** The financial supports from National Natural Science Foundation of China (NSFC Grant No. 52008373) are greatly acknowledged.

## References


1. Terazaghi, K. Theoretical soil mechanics. *John Wiley and Sons* **1965**.
2. Ladanyi, B.; Hoyaux, B. A study of the trap-door problem in a granular mass. *Canadian Geotechnical Journal* **1969**, *6*, 1–14.
3. Vardoulakis, I.; Graf, B.; Gudehus, G. Trap-door problem with dry sand: A statical approach based upon model test kinematics. *International Journal for Numerical and Analytical Methods in Geomechanics* **1981**, *5*, 57–78.
4. Evans, C.H. An examination of arching in granular soils. PhD thesis, Massachusetts Institute of Technology, 1983.
5. Dewoolkar, M.M.; Santichaianant, K.; Ko, H.Y. Centrifuge modeling of granular soil response over active circular trapdoors. *Soils and foundations* **2007**, *47*, 931–945.
6. Chevalier, B.; Combe, G.; Villard, P. Experimental and Numerical Study of the Response of Granular Layer in the Trap-door Problem. AIP Conference Proceedings. American Institute of Physics, 2009, Vol. 1145, pp. 649–652.
7. Costa, Y.D.; Zornberg, J.G.; Bueno, B.S.; Costa, C.L. Failure mechanisms in sand over a deep active trapdoor. *Journal of Geotechnical and Geoenvironmental Engineering* **2009**, *135*, 1741–1753.
8. Iglesia, G.R.; Einstein, H.H.; Whitman, R.V. Investigation of soil arching with centrifuge tests. *Journal of Geotechnical and Geoenvironmental engineering* **2014**, *140*, 04013005.
9. Zhao, Y.; Gong, Q.; Wu, Y.; Tian, Z.; Zhou, S.; Fu, L. Progressive failure mechanism in granular materials subjected to an alternant active and passive trapdoor. *Transportation Geotechnics* **2021**, *28*, 100529.
10. Heisen-Jen, T. A literature study of the arching effect. PhD thesis, Taipei: Taiwan University, 1990: 123–125.
11. Papamichos, E.; Vardoulakis, I.; Heil, L. Overburden modeling above a compacting reservoir using a trap door apparatus. *Physics and Chemistry of the Earth, Part A: Solid Earth and Geodesy* **2001**, *26*, 69–74.
12. Pardo, G.; Sáez, E. Experimental and numerical study of arching soil effect in coarse sand. *Computers and Geotechnics* **2014**, *57*, 75–84.
13. Rui, R.; van Tol, F.; Xia, Y.y.; van Eekelen, S.; Hu, G. Evolution of soil arching: 2D analytical models. *International Journal of Geomechanics* **2018**, *18*, 04018056.
14. Shukla, S.; Gaurav.; Sivakugan, N. A simplified extension of the conventional theory of arching in soils. *International Journal of Geotechnical Engineering* **2009**, *3*, 353–359.
15. AC01895560, A. *Code of practice for strengthened/reinforced soils and other fills*; BSi, 1995.
16. Gong, Q.; Zhang, R.; Zhou, S.; et al. Method for calculating loosening earth pressure around tunnels based on ellipsoid theory of particle flows. *Chin. J. Geotech. Eng* **2017**, *39*, 99–105.
17. Lai, F.; Chen, S.; Xue, J.; Chen, F. New analytical solutions for shallow cohesive soils overlying trench voids under various slip surfaces. *Transportation Geotechnics* **2020**, *25*, 100411.
18. Hewlett, W.; Randolph, M. Analysis of piled embankments. International Journal of Rock Mechanics and Mining Sciences and Geomechanics Abstracts. Elsevier Science, 1988, Vol. 25, pp. 297–298.
19. Adachi, T.; Kimura, M.; Kishida, K. Experimental study on the distribution of earth pressure and surface settlement through three-dimensional trapdoor tests. *Tunnelling and Underground Space Technology* **2003**, *18*, 171–183.
20. Li, L.; Aubertin, M.; Belem, T. Formulation of a three dimensional analytical solution to evaluate stresses in backfilled vertical narrow openings. *Canadian Geotechnical Journal* **2005**, *42*, 1705–1717.
21. Son, M. Three-dimensional expansion of the terzaghi arching formula considering inclined sliding surfaces and examination of its effects. *International journal of geomechanics* **2017**, *17*, 06016043.
22. Chevalier, B.; Otani, J. 3-D arching effect in the trap-door problem: A comparison between X-ray CT scanning and DEM analysis. In *GeoFlorida 2010: Advances in Analysis, Modeling & Design*; 2010; pp. 570–579.
23. Ma, Y.; Lü, X.; Huang, M. DEM study of the three dimensional effect of soil arching in piled-embankments. Civil Infrastructures Confronting Severe Weathers and Climate Changes Conference. Springer, 2018, pp. 36–44.
24. Liang, L.; Xu, C.; Chen, Q.; Chen, Q. Experimental and theoretical investigations on evolution of soil-arching effect in 2D trapdoor problem. *International Journal of Geomechanics* **2020**, *20*, 06020007.